High-Resolution EPR Spectroscopic Investigations of a Homologous Set of d^9-Cobalt(0), d^9-Rhodium(0), and d^9-Iridium(0) Complexes

Stephan Deblon,[a] Lorenz Liesum,[b] Jeffrey Harmer,[b] Hartmut Schönberg,[a] Arthur Schweiger,*[b] and Hansjörg Grützmacher*[a]

Abstract: The 17-electron complexes $[M(tropp^{ph})_2]$ ($M = Co^0$, Rh^0, Ir^0) were prepared and isolated (tropp = *trop*ylidene *p*hosphane). A structural analysis of $[Co(tropp^{ph})_2]$ revealed this complex to be almost tetrahedral, while the heavier homologues have more planar structures. Partially deuterated tropp complexes $[D_6][M(tropp^{ph})_2]$ were synthesised for M = Rh and Ir in order to enhance the resolution in the EPR spectra. This synthesis involves a fourfold intramolecular C–H activation reaction, whereby alkyl groups are transformed into olefins. Dihydrides were observed as intermediates for M = Ir. The electronic and geometric structures of all complexes $[M(tropp^{ph})_2]$ (M = Co, Rh, Ir) and $[D_6][M(tropp^{ph})_2]$ (M = Rh, Ir) were investigated by continuous wave (CW) and echo-detected EPR in combination with pulse ENDOR and ESEEM techniques. In accord with their planar structures, *cis* and *trans* isomers were detected for $[M(tropp^{ph})_2]$ ($M = Rh^0$, Ir^0) for which a dynamic equilibrium was established. The thermodynamic data show that the *cis* isomer is slightly preferred by $\Delta H^\circ = -4.7 \pm 0.3$ kJ mol^{-1} (M = Rh) and $\Delta H^\circ = -5.1 \pm 0.5$ kJ mol^{-1}; (M = Ir). The entropies for the process *trans*-$[M(tropp^{ph})_2] \rightleftharpoons$ *cis*-$[M(tropp^{ph})_2]$ are also negative [$\Delta S^\circ = -5 \pm 1.5$ J mol^{-1} (M = Rh); $\Delta S^\circ = -17 \pm 3.7$ J mol^{-1} (M = Rh)], indicating higher steric congestion in the *cis* isomers. The cobalt(0) and iridium(0) complexes show rather large *g* anisotropies, while that of the rhodium(0) complex is small (Co: $g_\parallel = 2.320$, $g_\perp = 2.080$; *cis*-Rh: $g_\parallel = 2.030$, $g_\perp = 2.0135$; *trans*-Rh: $g_\parallel = 2.050$, $g_\perp = 2.030$; *cis*-Ir: $g_\parallel = 2.030$, $g_\perp = 2.060$; *trans*-Ir: $g_\parallel = 1.980$, $g_\perp = 2.150$). The *g* matrices of $[M(tropp^{ph})_2]$ (M = Co, Rh) are axially symmetric with $g_\parallel > g_\perp$, indicating either a distorted square planar structure (SOMO essentially $d_{x^2-y^2}$) or a compressed tetrahedron (SOMO essentially d_{xy}). Interestingly, for $[Ir(tropp^{ph})_2]$ the inverse ordering, $g_\perp > g_\parallel$, is found; this cannot be explained by simple ligand field arguments and must await a more sophisticated analysis. The hyperfine interactions of the unpaired electron with the metal nuclei, phosphorus nuclei, protons, deuterons and carbon nuclei were determined. By comparison with atomic constants, the spin densities on these centres were estimated and found to be small. However, the good agreement of the distance between the olefinic protons and the metal centres determined from the dipolar coupling parameter indicates that the unpaired electron is primarily located at the metal centre.

Keywords: C–H activation · cobalt · EPR spectroscopy · iridium · organometallic radicals · phosphane ligands · rhodium

Introduction

Stable mononuclear open-shell organometallics are still comparatively unexplored and this is especially true for the late transition metals from periods 5 and 6.[1] While a number of cobalt(0) complexes have been investigated, the failure in characterising satisfactorily rhodium(0) and iridium(0) complexes may be due to the lack of suitable ligand systems to stabilise these species. On the other hand analytical tools also remained to be developed in order to analyse such compounds adequately.

The following selected complexes are relevant to this work and include the cobalt(0) complexes $[Co\{P(OMe)_3\}_4]$,[2a] $[Co(PMe_3)_2(olefin)_2]$[2b] and $[Co(CO)_4]$,[2d] the rhodium and iridium complexes $[Rh\{P(OiPr)_3\}_4]$,[3a,b] $[Rh(PPh_3)_4]$,[4], $[M(CO)(PPh_3)_3]$[5] (M = Rh, Ir), $[Rh(CO)_4]$,[2c] $[Rh(cod)_2]$,[6], and the recently prepared iridium complex $[Ir(dppf)_2]$ [dppf = 1,1′-bis(diphenylphosphanyl)ferrocene].[7] While the cobalt(0) complexes can generally be isolated, the rhodium(0) and iridium(0) complexes proved to be unstable and were mostly electrochemically generated and characterised as intermediates in solution. The carbonyls $[M(CO)_4]$ (M = Co, Rh, Ir) are only stable in noble gas matrices.[2c–f] Exceptions

[a] Prof. Dr. H. Grützmacher, Dr. S. Deblon, Dr. H. Schönberg
Laboratory of Inorganic Chemistry, ETH-Hönggerberg
8093 Zürich (Switzerland)
Fax: (41) 1-632-1090
E-mail: gruetzmacher@inorg.chem.ethz.ch

[b] Prof. Dr. A. Schweiger, Dr. L. Liesum, Dr. J. Harmer
Laboratory of Physical Chemistry, ETH-Zentrum
8092 Zürich (Switzerland)
Fax: (41) 1-632-1538
E-mail: schweiger@phys.chem.ethz.ch

  0947-6539/02/0803-0601 $ 17.50+.50/0

are the complexes $[Rh\{P(OiPr)_3\}_4]$[3a] and $[Ir(dppf)_2]$,[7] which were obtained as deep blue and green solids, respectively.

The structures of tetracoordinate d^9 species of the general formula $[ML_4]$ are interesting, because a distortion from a regular tetrahedral structure with a degenerate doublet ground state towards a structure with C_{3v} or D_{2d} symmetry is expected on the basis of the Jahn–Teller theorem.[8] In accord with this expectation, cobalt(0) complexes have tetrahedrally distorted structures (C_{3v}).[2a–c, 9, 10] However, little is known with certainty about the structures of the heavier congeners and some results are conflicting. For example, on the basis of EPR spectral data a square planar as well as a compressed tetrahedral structure (D_{2d}) were proposed for $[Rh\{P(OiPr)_3\}_4]$ by different groups.[3a,b] Distorted tetrahedral structures were also suggested for $[Rh(PPh_3)_4]$, $[M(CO)(PPh_3)_3]$ and $[Rh(CO)_4]$ (D_{2d}) in order to interpret the EPR data. Recently, such a distorted tetrahedral structure could be confirmed through an X-ray diffraction study of the complex $[Ir(dppf)_2]$ (the angle ϕ defined by the intersection of the planes running through the phosphorus centres of one dppf ligand and the metal centre amounts to 74°; tetrahedron: $\phi = 90°$, square planar: $\phi = 0/180°$).[7] On the other hand, the EPR data for $[Rh(cod)_2]$ are in better agreement with a structure close to square planar.

Recently, we developed the tropp ligand (tropp = *tropyl*idene *p*hosphanes),[11] which contains a phosphane and an olefin binding unit within a rigid concave framework (Scheme 1).

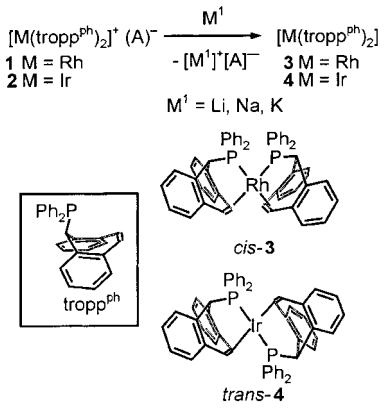

Scheme 1. Synthesis of the 17-electron $[M(tropp^{ph})_2]$ complexes (M = Rh: **3**, M = Ir: **4**).

This ligand allows the high-yield synthesis of the stable mononuclear paramagnetic 17-electron metal(0) complexes $[Rh(tropp^{ph})_2]$ (**3**)[12] and $[Ir(tropp^{ph})_2]$ (**4**) by electrochemical or chemical reduction of their corresponding 16-electron cationic precursor complexes **1** and **2**.[13] The complexes have distorted planar structures and, in accord with this description, *cis* and *trans* isomers are to be expected for a complex of the type $[MA_2B_2]$. Indeed, single-crystal X-ray structure analyses showed **3** to be the *cis* isomer, while for **4** the *trans* isomer was observed. The *cis*-configured rhodium(0) complex *cis*-**3** is slightly more distorted ($\phi = 41°$) than the *trans* isomer *trans*-**4** of the iridium(0) complex ($\phi = 32°$).

Here we wish to investigate the complete series of d^9-$[M(tropp^{ph})_2]$ complexes with the synthesis of d^9-$[Co(tropp^{ph})_2]$. Thereby, the characterization of a strictly homologous set of tetracoordinate, d^9 valence electron configured, organometallic complexes by using continuous wave (CW) and echo-detected EPR, and two-dimensional ENDOR and ESEEM methods became possible.[14]

Results

Syntheses: Our usual syntheses start with the cationic d^8-$[M(tropp^{ph})_2]^+$ complexes **1** (M = Rh) or **2** (M = Ir), which can be easily reduced with alkali metals to the neutral d^9-$[M(tropp^{ph})_2]$ complexes **3** (M = Rh) or **4** (M = Ir), respectively (M^1 = Li, Na, K) (Scheme 1 vide supra). Interestingly, the attempted synthesis of the 16-electron complex d^8-$[Co(tropp^{ph})_2]^+$ failed.

Although the mono tropp complex **6** can be easily prepared from **5**, further treatment with $tropp^{ph}$ in presence of KPF_6 initiated a redox reaction and gave the neutral paramagnetic cobalt(0) complex d^9-$[Co(tropp^{ph})_2]$ (**7**) as the only product soluble in organic solvents (Scheme 2, top). As a further

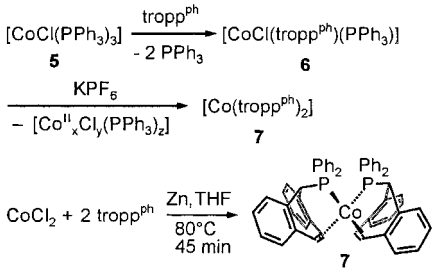

Scheme 2. Syntheses of $[CoCl(tropp^{ph})(PPh_3)]$ (**6**) and $[Co(tropp^{ph})_2]$ (**7**).

by product, a brown insoluble material (presumably mixed cobalt(II) chloride PPh_3 complexes) was obtained; we did not characterise this material any further. In a direct way and with excellent yield (> 90 %), complex **7** is prepared by heating a mixture of anhydrous $CoCl_2$ (or $CoBr_2$) with two equivalents of $tropp^{ph}$ in the presence of zinc powder (Scheme 2, bottom). Unfortunately, complex **7** forms very thin orange plates which allowed only a poorly refined structure determination using X-ray diffraction data.[15] However, the expected tetrahedral structure was unequivocally confirmed. The sum of the six bond angles which are enclosed by the phosphorus atoms and the centroids (Ct) of the coordinated double bonds amounts to about 657.8° and the intersection angle ϕ between the planes running through the metal, the phosphorus and the C=C centroid of each $tropp^{ph}$ ligand is 86° (expected values for a tetrahedron 658.2° and 90°, respectively). The molecular stucture of **6** was determined with sufficient precision and is shown in Figure 1. Selected bond lengths and angles are given in the caption. All distances are within the range commonly observed for cobalt(I) complexes.[16] In this complex the sum of the six bond angles that define the tetrahedral coordination sphere around the cobalt atom amounts 656.3°, that is, the structures of **6** and **7** are very similar.

0947-6539/02/0803-0602 $ 17.50+.50/0 *Chem. Eur. J.* **2002**, *8*, No. 3

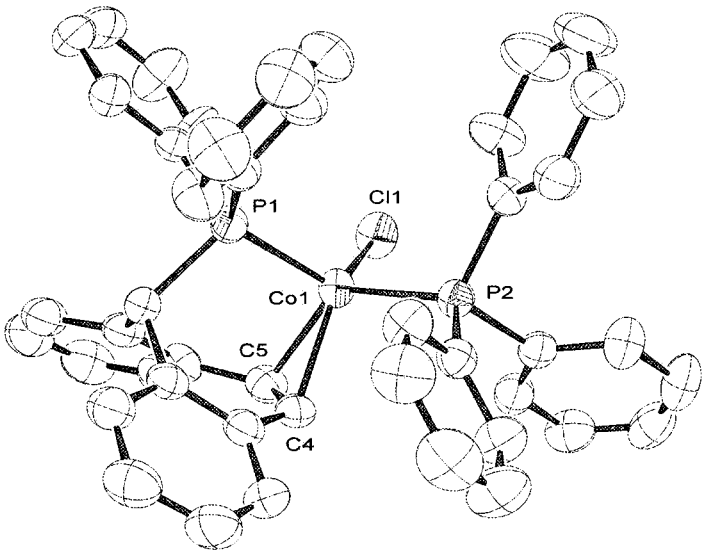

Figure 1. Molecular structure of **6**. Selected bond lengths [Å] and angles [°]; Ct indicates the centroid of the coordinated C4=C5 bond: Co1–C5 2.095(4), Co1–C4 2.170(5), Co–Ct 2.016, Co1–Cl1 2.2148(14), Co1–P1 2.2699(13), Co1–P2 2.3341(13); C5-Co1-C4 38.1(2), C5-Co1-Cl1 103.09(14), C4-Co1-Cl1 134.94(14), C5-Co1-P1 94.90(13), C4-Co1-P1 93.23(13), Cl1-Co1-P1 117.30(5), C5-Co1-P2 125.44(14), C4-Co1-P2 91.22(14), Cl1-Co1-P2 106.42(5), P1-Co1-P2 110.15(5).

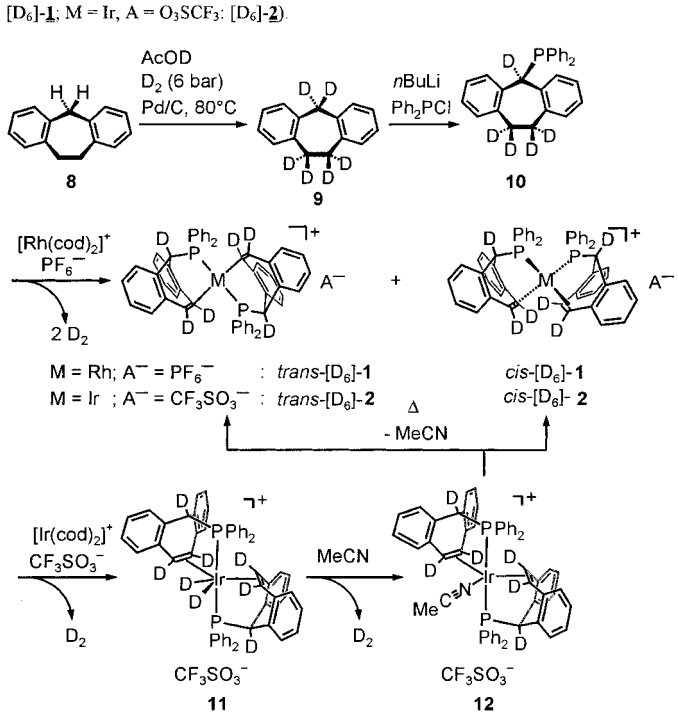

Scheme 3. Syntheses of the partially deuterated complexes $[D_6][M(tropp^{ph})_2]^+A^-$ (M = Rh, A = PF_6: $[D_6]$-**1**; M = Ir, A = O_3SCF_3: $[D_6]$-**2**).

We were in the fortunate position to have three different complexes at hand in which:

1) Only the metal centre varies along a column (i.e. the complexes are electronically strictly isovalent).
2) Each of them represents one of the three possible isomers of a $[MA_2B_2]$ complex (i.e. a tetrahedron and the *cis* and *trans* isomer of a square planar complex)
3) All ligand nuclei in the proximity of the paramagnetic metal centre have a nuclear spin I = ½ (^{13}C in 1% natural abundance)

This enabled us to plan a detailed EPR investigation using various techniques in order to gain insight into the electronic structure of these d^9-$[M(tropp^{ph})_2]$ complexes. As a first step, the synthesis of a partially deuterated tropp ligand was envisioned to enhance the resolution of the EPR spectra because the hyperfine coupling of deuterium is 6.5 times less than the corresponding proton coupling. The deuteration also simplifies the interpretation of the ENDOR and ESEEM spectra.

The synthesis begins with an H/D exchange reaction of the benzyl positions in dibenzosuberone **8** by using a pressure of 5 bar D_2 and palladium charcoal as a catalyst in $[D_1]$acetic acid. After two repetitions, this reaction furnishes a 90% yield of a 93% deuterated product **9** (Scheme 3, top).

Lithiation occurs selectively in the activated bis(benzyl) position and after reaction with Ph_2PCl the $[D_5]$dibenzo[a,d]-cycloheptyl phosphane **10** was obtained in about 75% yield. The final and crucial step in our synthesis was the dehydro-(deutero)genation of **10**. Remarkably, this reaction proceeds smoothly in THF at 80 °C with $[Rh(cod)_2][PF_6]$ (Scheme 3, middle) or $[Ir(cod)_2][O_3SCF_3]$ (Scheme 3, bottom), to give either the cationic rhodium(I) complex $[D_6]$-**1** after 16 h or the iridium(I)dideuteride complex **11**[17] after 30 min in good to excellent yields. To our knowledge, this is a rare case for the syntheses of stable diolefin complexes by using a dehydrogenation sequence involving four intramolecular C–H activations of alkyl groups.[18] From dideuteride complex **11**, the second equivalent D_2 is liberated easily by adding acetonitrile to the reaction solution. The resulting pentacoordinate colourless complex **12** was dried in vacuum, whereby the tetracoodinate 16-electron complexes $[D_6]$-**1** and $[D_6]$-**2** formed as mixtures of *cis* and *trans* isomers in which the latter prevails (*trans*/*cis*-**1**: 80/20; *trans*/*cis*-**2**: 88/12).[19] The complexes $[D_6]$-**1** and $[D_6]$-**2** were reduced with potassium or lithium metal, respectively, in THF to give almost quantitatively the deuterated paramagnetic complexes $[D_6]$-**3** and $[D_6]$-**4** (c.f. Scheme 1).

EPR spectroscopy: The electronic and geometric structure of the complexes $[M(tropp^{ph})_2]$ (M = Co, Rh, Ir) and $[D_6][M(tropp^{ph})_2]$ (M = Rh, Ir) was investigated by continuous wave (CW) and echo-detected EPR in combination with pulse ENDOR and ESEEM techniques.[14] The *g* values as well as the metal and phosphorus hyperfine couplings of the three complexes together with the corresponding data of related compounds reported in the literature are listed in Table 1.

EPR spectra: Figure 2a shows the X-band CW EPR spectra of $[Co(tropp^{ph})_2]$ in THF recorded at room temperature (upper trace) and in a frozen THF at 120 K (lower trace). The tumbling of $[Co(tropp^{ph})_2]$ at room temperature is not fast enough to fully average the large *g* anisotropy. The Q-band

Table 1. Experimental EPR parameters of the $[M(tropp^{ph})_2]$ complexes **7** (M = Co), *cis*/*trans* **3** (M = Rh), and *cis*/*trans* **4** (M = Ir) and of some other Co^0, Rh^0, and Ir^0 complexes. Hyperfine couplings A in MHz.

	$g_\parallel$	$g_\perp$	g_{iso}	$\lvert A_\parallel \rvert$ (^{31}P)	$\lvert A_\perp \rvert$ (^{31}P)	$\lvert A_{iso} \rvert$ (^{31}P)	$\lvert A_\parallel \rvert$ (M)	$\lvert A_\perp \rvert$ (M)	$\lvert A_{iso} \rvert$ (M)	Ref.
$[Co(tropp^{ph})_2]$	2.320	2.080		80 ± 10	70 ± 10		140	70	–	this work
$[Co\{P(OMe)_3\}_4]$	2.149	2.099		312	240[b]		216	111	–	[2a]
$[Co(CO)_4]$	2.007	2.128		–	–	–	174	175	–	[2d]
cis-$[Rh(tropp^{ph})_2]$	2.030	2.0135	2.0195	80	65	69.5	20	16	17	this work
trans-$[Rh(tropp^{ph})_2]$	2.050	2.030	2.0370	55	40	45	23	19	20	this work
$[Rh\{P(OiPr)_3\}_4]$[a]	2.105, 2.016, 2.011			236, 260, 253		< 15	< 50	–	–	[3a]
$[Rh(CO)_4]$	2.015	2.002		–	–	–	< 15	24	–	[2c]
cis-$[Ir(tropp^{ph})_2]$	2.030	2.060		< 80	< 80	–	–		–	this work
trans-$[Ir(tropp^{ph})_2]$	1.980	2.150		< 80	< 80	–	–		–	this work
$[Ir(dppf)_2]$	2.190	2.060		–	–	–	–		–	[7]

[a] Note that a different interpretation of EPR data was given by Pilloni et al. who suggested a more planar structure in ref. [3b]. [b] The original literature cites a value of 2400 which we suspect is a typo.

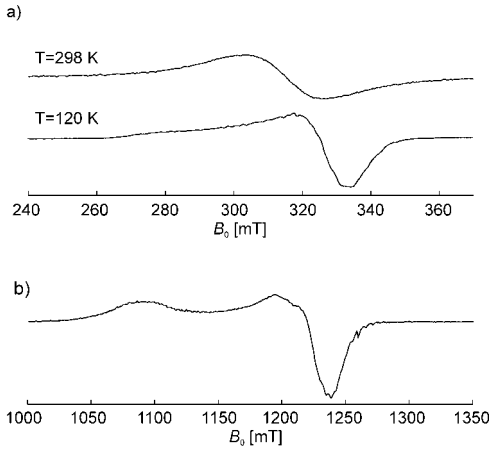

Figure 2. CW EPR spectra of $[Co(tropp^{ph})_2]$ in THF. a) X-band at 298 K (upper trace) and 120 K (lower trace). b) Q-band at 120 K.

CW EPR spectrum measured at 120 K is shown in Figure 2b. Hyperfine couplings are not resolved in these EPR spectra.

Figure 3 shows the room-temperature CW EPR X-band spectra of $[Rh(tropp^{ph})_2]$ (upper trace) and $[D_6][Rh(tropp^{ph})_2]$ (middle trace) in THF (a) and the Q-band spectra of $[D_6][Rh(tropp^{ph})_2]$ (upper trace) in THF (b), together with the corresponding simulations (lower trace). The rhodium(0) complexes have a small g anisotropy and are isotropic in solution.

The resolution of the solution spectra is enhanced by a deuteration of the olefinic protons as is demonstrated by comparing the two experimental spectra depicted in Figure 3a. Figure 3a and b also indicate that two isomers (labelled by **A** and **B**) exist with spectra that are completely separated at Q-band frequencies (centre field position of species **A**: $B_0 = 1237$ mT; species **B**: $B_0 = 1247$ mT). From the Q-band spectrum, the isotropic g values of the two isomers are found to $g^A_{iso} = 2.0370$ and $g^B_{iso} = 2.0195$.

To determine the anisotropic interactions, frozen solution EPR spectra of $[D_6][Rh(tropp^{ph})_2]$ were measured at four different microwave frequencies; they are shown in Figure 3c – f together with the corresponding simulations. Echo-detected EPR spectra were recorded at 20 K at S-band (c), Q-band (first derivative displayed) (e) and W-band frequencies (f), and CW EPR spectra were measured at 90 K at X-band frequencies (d). The small anisotropy of the axial g matrix is only resolved at W-band frequency at which the $g_\parallel$ position of both complexes and the $g_\perp$ position of complex **B** could be distinguished. The magnetic parameters of the two

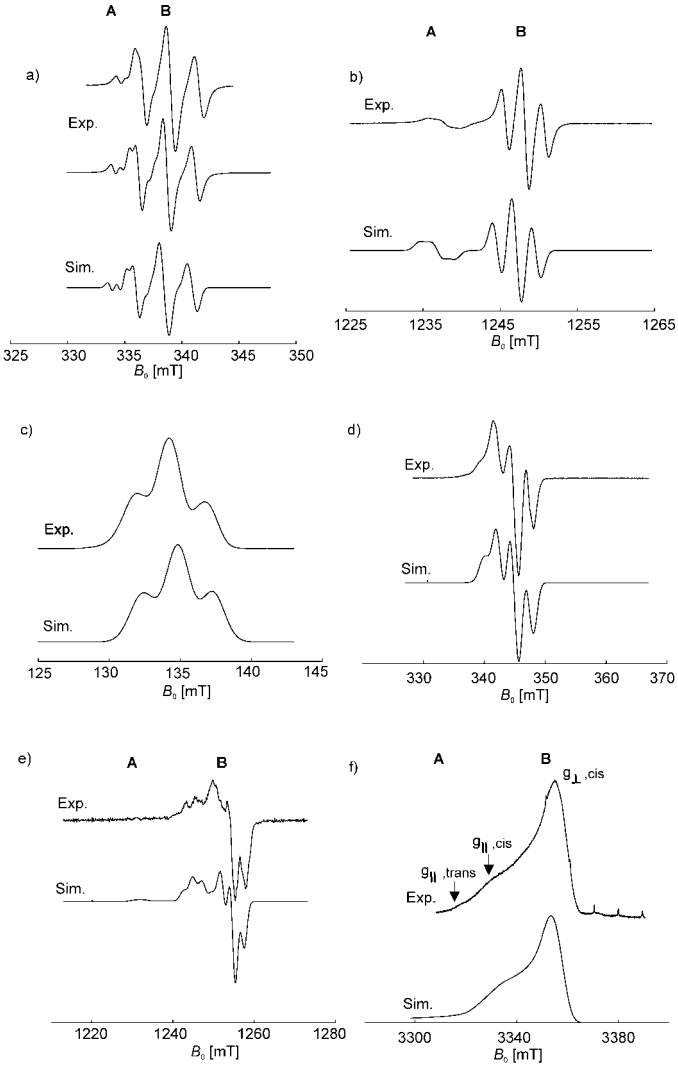

Figure 3. Experimental (Exp.) and simulated (Sim.) EPR spectra of $[Rh(tropp^{ph})_2]$. a) X-band CW EPR spectra of $[Rh(tropp^{ph})_2]$ in $[D_8]$THF (upper trace) and $[D_6][Rh(tropp^{ph})_2]$ in THF (middle trace) at 298 K. b) Q-band CW EPR spectra of $[D_6][Rh(tropp^{ph})_2]$ in THF at 298 K. c – f) EPR spectra of $[D_6][Rh(tropp^{ph})_2]$ in THF by using S-band echo-detected EPR at 20 K (c), X-band CW EPR at 90 K (d), Q-band echo-detected EPR at 20 K (first derivative) (e) and W-band echo-detected EPR at 20 K (f).

  0947-6539/02/0803-0604 $ 17.50+.50/0 *Chem. Eur. J.* **2002**, *8*, No. 3

isomers obtained from simulations of the frozen solution spectra are given in Table 1.

Figure 4a shows the X-band CW EPR spectrum of $[D_6]$-$[Ir(tropp^{ph})_2]$ in THF recorded at 298 K (upper trace) and the echo-detected EPR spectrum measured at $T = 20$ K (middle trace) together with the numerical simulation (lower trace).

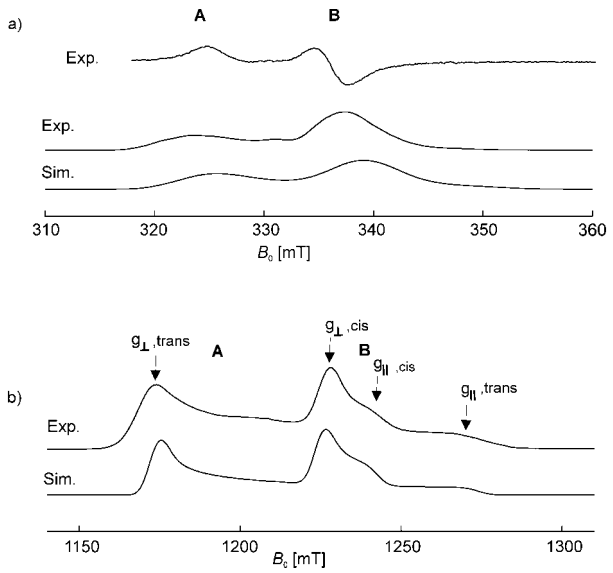

Figure 4. Experimental (Exp.) and simulated (Sim.) EPR spectra of $[Ir(tropp^{ph})_2]$ in THF. a) X-band CW EPR at 298 K (upper trace) and echo-detected EPR at 20 K (middle trace). b) Q-band echo-detected EPR at 20 K.

Again, two isomers, **A** and **B**, can be identified, which are clearly distinguishable in the echo-detected EPR Q-band spectrum ($T = 20$ K) shown in Figure 4b. The spectra of both isomers are comparable in intensity and have axially symmetric g matrices with $g_\perp > g_\parallel$, in contrast to Co^0 and Rh^0 where $g_\parallel > g_\perp$.

Isomer assignment and dynamic equilibrium: The dynamic equilibrium of the two isomers found in the rhodium and iridium complex was studied by measuring the temperature dependence of the solution EPR spectra of the two compounds. Figure 5 shows the CW EPR spectra of the rhodium complexes $[D_6]$-**3** (a) and the iridium complexes $[D_6]$-**4** (b) as a function of temperature. The corresponding simulated spectra of species **A** and **B** are shown in Figure 5c and d, respectively. In the iridium spectra the g anisotropy is not fully averaged out, so that for the determination of the intensity ratios of the spectra of **A** and **B**, powder spectra simulated with adapted effective g values where used.

A comparison of the value $g = 2.02$ obtained from the EPR spectrum of the polycrystalline rhodium(0) complex *cis*-**3**[12] with the isotropic g values of **A** and **B** obtained from the solution spectra indicates that the signals of species **B** correspond to the *cis* isomer, and, consequently, that of species **A** to the *trans* isomer. From the principal values $g_\parallel$ and $g_\perp$ of the two isomers of the iridium(0) complex **4** (Table 1), the isotropic g values were calculated to be $g_{iso}^{A} = 2.093$ and $g_{iso}^{B} = 2.050$. The value $g_{iso} = 2.09$ obtained from $g_\parallel$ and $g_\perp$ of the spectrum of a polycrystalline sample of complex *trans*-**4**[13] again allowed the unambiguous assignment of species **B** to the *cis* isomer and of species **A** to the *trans* isomer. For $[Co(tropp^{ph})_2]$ **7**, only one species was observed in agreement with the assumed tetrahedral symmetry.

Metal and phosphorus hyperfine couplings: The hyperfine couplings of the metal ions were derived from simulations of the EPR spectra and/or from direct measurements using pulse ENDOR. The Davies–ENDOR spectra of $[Co(tropp^{ph})_2]$ measured at different observer positions and the corresponding simulations are shown in Figure 6. The cobalt hyperfine matrix and g matrix were found to be approximately coaxial. The cobalt quadrupole interaction was not resolved.

For the *trans* isomer **A** the isotropic rhodium hyperfine coupling $A_{iso} = 21$ MHz could be derived from the CW EPR spectrum in solution. The anisotropic rhodium hyperfine couplings of the *cis* isomer **B** were determined by using two-dimensional Mims–ENDOR spectroscopy (Figure 7),[20, 14] which correlates the hyperfine frequencies, ν_{hf}, with the ENDOR frequencies, ν_{ENDOR}. The ridges are separated by twice the Zeeman frequency $\nu_I(Rh)$ of rhodium and can thus unambiguously be assigned to this nucleus. The anisotropy of the hyperfine coupling was examined by orientation-selective

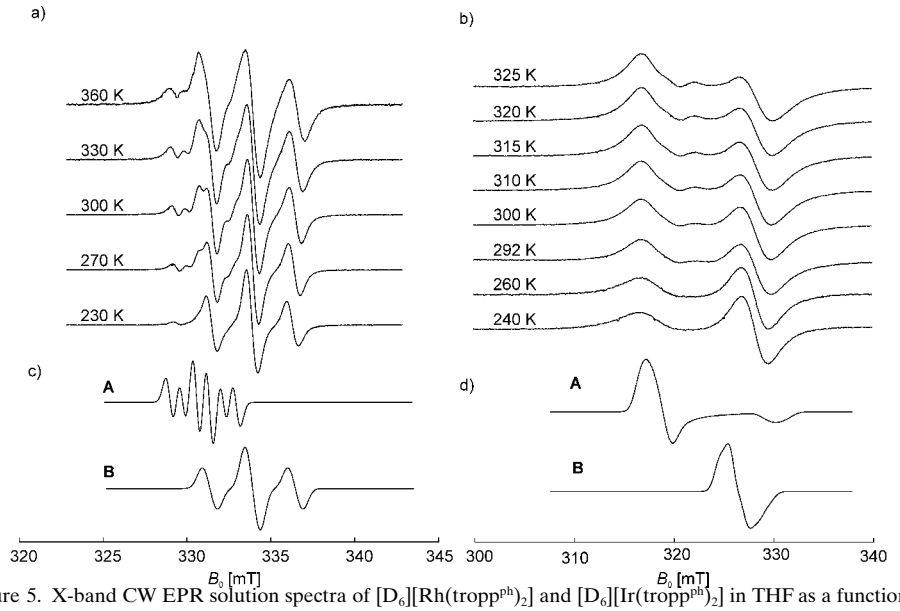

Figure 5. X-band CW EPR solution spectra of $[D_6][Rh(tropp^{ph})_2]$ and $[D_6][Ir(tropp^{ph})_2]$ in THF as a function of temperature. a) Spectra of $[D_6][Rh(tropp^{ph})_2]$ between 230 K and 360 K. b) Spectra of $[D_6][Ir(tropp^{ph})_2]$ between 240 K and 325 K. c) Simulated spectra of the *trans*-(**A**) and *cis*-(**B**) isomers of $[D_6][Rh(tropp^{ph})_2]$. d) Simulated spectra of the *trans*-(**A**) and *cis*-(**B**) isomers of $[D_6][Ir(tropp^{ph})_2]$.

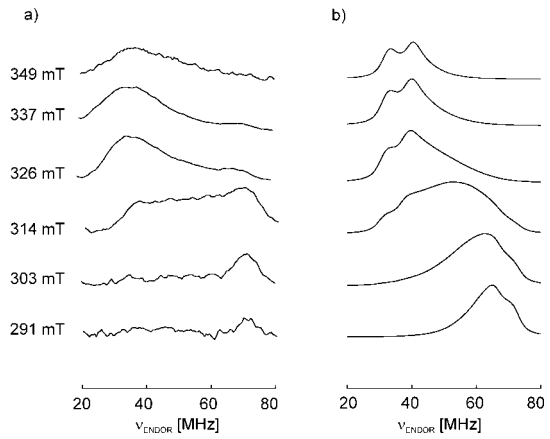

Figure 6. X-band Davies–ENDOR spectra of $[Co(tropp^{ph})_2]$ in THF at different observer positions and $T = 20$ K (fields are indicated in the figure). a) Experimental spectra. b) Simulations.

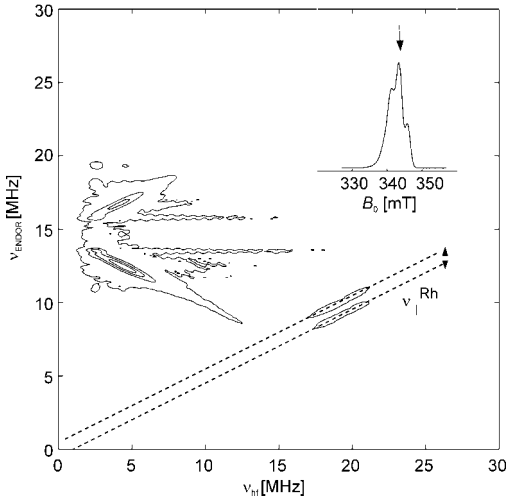

Figure 7. Two-dimensional Mims–ENDOR spectrum of $[Rh(tropp^{ph})_2]$. The dashed lines are separated by $2\nu_I(Rh)$ and cross the ν_{hf} and ν_{ENDOR} axes at $\nu_I(Rh)$. Inset: EPR spectrum, the arrow indicates the observer position used for the ENDOR experiment.

Davies–ENDOR measurements (not shown). The iridium hyperfine coupling, which based on the small gyromagnetic factor of the iridium nucleus is expected to be around 4 MHz, could not be observed experimentally.

The phosphorus hyperfine data could most accurately be determined for the rhodium complexes. For both isomers, the isotropic hyperfine couplings could be obtained from the solution spectra and the anisotropic coupling from simulations of the frozen solution spectra. For the cobalt complex the hyperfine structure in the X-band spectrum, which is due to hyperfine couplings of the two phosphorus nuclei and the hyperfine interaction of the cobalt, could not be fitted exactly by simulation. However, estimates for the phosphorus and the cobalt couplings derived from the ENDOR spectra matched very well to the width of the $g_{\|}$ and $g_{\perp}$ positions in the spectrum. For the two iridium complexes only upper limits of the phosphorus hyperfine couplings could be obtained.

Hyperfine interactions of surrounding protons, deuterons and carbon atoms: The hyperfine interactions of the surrounding protons and carbon nuclei of $[Rh(tropp^{ph})_2]$ and $[D_6][Rh(tropp^{ph})_2]$ were obtained from HYSCORE spectra[23, 14] measured at X-band at $T = 20$ K. The couplings of the olefinic protons could be determined by recording HYSCORE spectra of both the fully protonated complex **3** and the partially deuterated complex $[D_6]$-**3**. The spectrum of complex **3** is shown in Figure 8a. The proton spectrum shows two types of ridges, labelled 1 and 2.

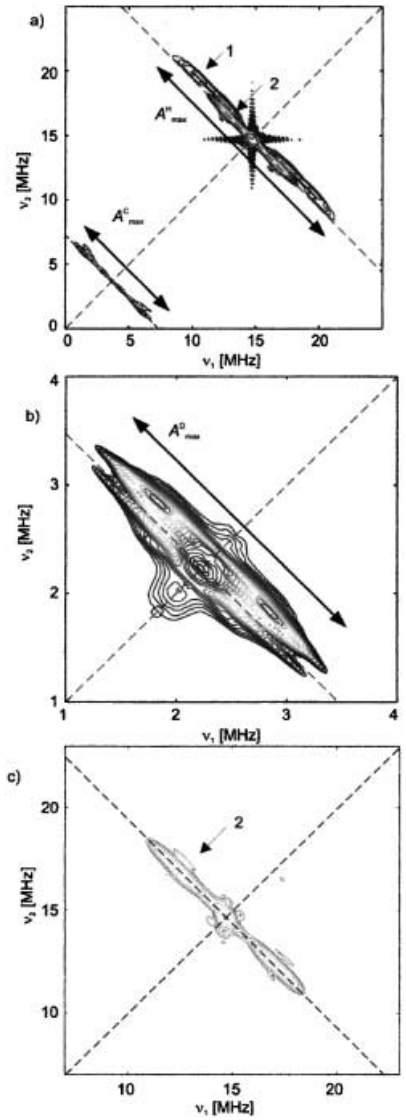

Figure 8. X-band HYSCORE spectra of the rhodium complex recorded at 20 K in THF. a) Spectrum of $[Rh(tropp^{ph})_2]$. b) Deuterium spectrum of $[D_6][Rh(tropp^{ph})_2]$. c) Proton spectrum of $[D_6][Rh(tropp^{ph})_2]$. The double-sided arrows indicate the maximum hyperfine couplings. The anti-diagonals cross the diagonal at (ν_I^H, ν_I^H), (ν_I^C, ν_I^C) and (ν_I^D, ν_I^D).

The maximum proton hyperfine coupling of 12 MHz, which is assigned to the olefinic protons, matches very well with the deuteron coupling of 2.1 MHz shown in Figure 8b. In the proton HYSCORE spectrum of $[D_6][Rh(tropp^{ph})_2]$ (Figure 8c) the ridges 1 with the large hyperfine coupling are missing; this indicates that these signals have to be assigned to the olefinic protons.

The dipolar coupling constant $T = 4.3$ MHz of the olefinic protons was obtained from a proton combination-peak

  0947-6539/02/0803-0606 $ 17.50+.50/0 *Chem. Eur. J.* **2002**, *8*, No. 3

experiment.[14] The distance r between the rhodium centre and the protons can be determined under the assumption that the point-dipole interaction described by Equation (1)[24] is valid.

$$T=\frac{\mu_o}{4\pi}\frac{g g_n \beta_e \beta_n}{r^3 h} \quad (1)$$

We found a value of 265 pm, which is in excellent agreement with distances determined by X-ray analysis.[12, 13] Finally, hyperfine couplings of ^{13}C nuclei (in natural abundance!) up to 5 MHz could be observed in the HYSCORE spectrum (Figure 8a).

Discussion

In this section a brief discussion of the experimental EPR data is given. A detailed analysis of the magnetic parameters and of the spin density distributions, complemented by results obtained from density functional theory, is in preparation.

Dynamic equilibrium of *cis* and *trans* $[D_6][M(tropp^{ph})_2]$ (M = Rh, Ir): For each temperature, the intensity ratio of the spectra of the two isomers was determined by fitting the simulated to the experimental spectra. From a van't-Hoff plot ($\ln K$ vs $1/T$) the thermodynamic data (ΔH°, ΔS°) were obtained. Most likely, the *trans* $\rightleftharpoons$ *cis* isomerisation proceeds in an intramolecular way via a low-lying tetrahedral transition state.

The thermodynamic data show that the *cis* isomer of the neutral d^9-$[M(tropp^{ph})_2]$ complexes (M = Rh, Ir) is slightly preferred (*trans*-**3** $\rightleftharpoons$ *cis*-**3**: $\Delta H^\circ = -4.7 \pm 0.3$ kJ mol^{-1}; *trans*-**4** $\rightleftharpoons$ *cis*-**4**: $\Delta H^\circ = -5.1 \pm 0.5$ kJ mol^{-1}). This is in contrast to the cationic d^8-$[M(tropp^{ph})_2]^+$ complexes in which the *trans* isomer is dominant (vide supra), but for which thermal isomerisation, a formally spin-forbidden process,[22] does not occur in non or weakly coordinating solvents. However, the entropy is also negative for the *trans* $\rightarrow$ *cis* isomerisation process displayed in Scheme 4 (**3**: $\Delta S^\circ = -5 \pm 1.5$ J mol^{-1}; **4**: $\Delta S^\circ = -17 \pm 3.7$ J mol^{-1}) leading to *trans*/*cis* mixtures of 22/78

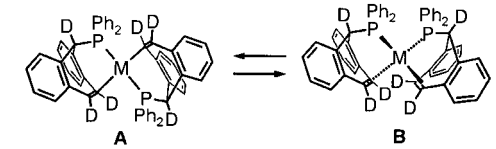

Scheme 4. *trans* $\rightleftharpoons$ *cis* isomersation of paramagnetic d^9-$[M(tropp^{ph})_2]$ complexes (M = Rh, Ir).

and 50/50 for **3** and **4**, respectively, at room temperature. Negative entropies are expected for the isomerisation process, because the *cis* isomer is sterically more congested leading to a restriction of conformational freedom as was evidenced by NMR experiments for other cationic $[Rh(tropp)_2]^+$ complexes with a *cis* configuration.[1b] Note that the anionic d^{10}-$[M(tropp^{ph})_2]^-$ complexes are surprisingly *nonfluxional* on the NMR timescale and always show a distorted *cis* structure ($\phi \approx 52^\circ$).[1b, 12, 13] Clearly in the series, *trans*/*cis*-d^8-$[M(tropp^{ph})_2]^+$ (rigid) + $e^- \rightarrow$ *cis/trans*-d^9-$[M(tropp^{ph})_2]$ (fluxional) + $e^- \rightarrow$ *cis*-d^{10}-$[M(tropp^{ph})_2]^-$ (rigid) (M = Rh, Ir), a preference for placing electronically alike ligands in the *cis* positions with increasing d-valence electron configuration on the metal centre comes to the fore (stereoelectronic *cis* influence). The origin for this behaviour may be an increasing metal-to-ligand back-donation.

Interestingly, the dynamic behaviour of $[M(tropp^{ph})_2]$ is distinct from the one found for the rhodium(0) complex $[Rh(dppe)_2]$[21] (dppe = diphenylphosphinoethane). In this compound either a pairwise lengthening and shortening of the Rh–P bonds or an angular distortion to a pseudo-trigonal bipyramidal structure of C_2 symmetry was proposed to account for the observation that the symmetric five-line pattern in the EPR spectrum at higher temperatures changes to a spectrum showing couplings to pairwise inequivalent phosphorus nuclei upon cooling. Also, the intensity of the EPR signals decreased with decreasing temperature which points to the formation of a diamagnetic species, that is, either a dimer, $[Rh_2(dppe)_4]$, or an intimate ion pair, $[Rh(dppe)_2]^+[Rh(dppe)_2]^-$.

***g* anisotropy and spin densities**: The g matrices of $[M(tropp^{ph})_2]$ (M = Co, Rh) are axially symmetric with $g_\parallel > g_\perp$, indicating that the geometry of the complex is either distorted square planar, in which the unpaired electron essentially occupies the $d_{x^2-y^2}$ orbital, or corresponds to a compressed tetrahedron with the unpaired electron in the d_{xy} orbital. Knowing the solid-state structures in combination with the observation that *cis* and *trans* isomers were observed for $[Rh(tropp^{ph})_2]$, we are quite certain that the first case applies to the rhodium(0) complex. Life is not so easy with $[Co(tropp^{ph})_2]$ (**7**). While the solid-state structure clearly points to the interpretation that **7** has a tetrahedral structure, we cannot exclude that in solution a more planar structure prevails. In that case, the *cis* and *trans* isomers equilibrate very rapidly or—more likely—only one of them is formed and is rigid on the EPR timescale. In either case, the expressions for the g principal values to first order in λ/E are given by Equations (2) and (3):

$$g_\parallel = g_e + \frac{8|\lambda|}{E} \quad (2)$$

$$g_\perp = g_e + \frac{2|\lambda|}{E'} \quad (3)$$

where λ is the spin-orbit coupling constant, and E and E' are the energy separation between the $d_{x^2-y^2}$ and the d_{xy} orbital, and between the $d_{x^2-y^2}$ and the $d_{xz,yz}$ orbitals, respectively. Note, that Equations (2) and (3) are only useful providing λ/E is small. The g anisotropy of the cobalt complex is found to be much larger than the one of the two rhodium complexes. With the spin-orbit coupling constants $\lambda_{Rh} = -968$ cm^{-1} and $\lambda_{Co} = -517$ cm^{-1} for the free ions of Rh^0 and Co^0, this indicates that E and E' are much larger for rhodium than for cobalt. One may use the very large g anisotropy as an argument to propose a more planar structure for **7** in solution. Because E should be significantly larger than E' in a compressed tetrahedron, the $|\lambda|/E$ term does not add much to $g_\parallel$ despite its factor 8, while

the contribution to $g_\perp$ remains significant. As a net effect, a medium g anisotropy may result; this is indeed observed for $[Co\{P(OMe)_3\}_4]$ (see Table 1), which is likely to have the structure of a tetrahedron.[2a] On the other hand, E and E' are less different for a more square-planar structure and hence $g_\parallel$ should be significantly larger than $g_\perp$. Interestingly, the ratio of the deviations of $g_\parallel$ (2.320) and $g_\perp$ (2.080) from the g value of the free electron, g_e (2.00/23), equals almost precisely 4, indicating that E and E' are about equal and giving evidence for a more planar structure of **7**. A second argument for this assumption is the observation of rather similar phosphorus hyperfine couplings ($\sim$ 80 MHz) for all tropp complexes, which also implies similar structures. We assume that mixing of the orbitals $3d_{x^2-y^2}$ and $4p_z$ in the cobalt case, and $4d_{x^2-y^2}$ and $5p_z$ in the rhodium case, resulting in hybridised orbitals which are better directed towards the phosphorus atoms in a distorted square plane, accounts for the medium sized couplings.[30] For a perfectly planar structure larger hyperfine couplings are expected.

In contrast to the cobalt and rhodium complex, in both *cis*- and *trans*-$[Ir(tropp^{ph})_2]$ $g_\perp$ is larger than $g_\parallel$. In this case, one would conclude that the unpaired electron predominantly occupies the d_{z^2} orbital according to ligand field theory. The corresponding expressions for the principal g values are given by Equations (4) and (5):

$$g_\parallel = g_e \tag{4}$$

$$g_\perp = g_e + \frac{6|\lambda|}{E} \tag{5}$$

where E is the energy separation between d_{z^2} and $d_{xz,yz}$.

The same observation has been made for $[Co(CO)_4]$.[2d, 31] In this complex a larger hyperfine interaction to one ^{13}C nucleus and weak interactions to the other three ^{13}C was observed which indicates C_{3v} symmetry. However, this symmetry can be excluded for the $[Ir(tropp^{ph})_2]$ complex and for the moment we cannot explain the data with simple ligand field arguments in which the mixing of the d orbitals is neglected.

The spin densities can roughly be estimated by comparing the measured hyperfine couplings with those computed for the free ions.[25] The spin densities on the s orbitals of the ligand nuclei were calculated from the isotropic hyperfine couplings obtained from the solution spectra or from the anisotropic couplings using the expression $A_{iso} = (A_\parallel + 2A_\perp)/3$. We found that for the Co^0 and Rh^0 complexes about 1 % of the spin density resides on the s orbitals of the two phosphorus centres (0.5 % each). For the Rh^0 complex about 0.5 % resides on the s orbitals of the four olefinic carbon centres, and about 2 % on the four olefinic protons. The spin density on the p orbitals of the two phosphorus centres is estimated from the dipolar part of the hyperfine couplings to be about 4 %.

From the hyperfine data, a spin density of only about 2–5 % is found for Co^0 and Rh^0. On the other hand the absence of a large spin density on the ligands and the good agreement of the distance between the olefinic protons and the rhodium centre determined from the dipolar coupling parameter indicates that the unpaired electron is primarily located at the metal centre. A possible explanation for the small spin density on Co^0 and Rh^0 is that direct spin density in the higher lying orbitals and spin polarization of the lower lying core orbitals counterbalance, resulting in the observed small hyperfine couplings for the metals.[26] This is in agreement with the above-mentioned hybridised orbitals, since the contributions of the $d_{x^2-y^2}$ and p_z orbitals to the metal hyperfine interactions are opposite in sign and can cancel each other to a great extent.

Conclusion

In summary, the double dehydrogenation of two alkyl groups was the key step in the synthesis of paramagnetic d^9-$[D_6][M(tropp^{ph})_2]$ complexes (M = Co, Rh, Ir) containing two deuterated olefinic units. These allowed a detailed investigation by state-of-the-art high-resolution EPR spectroscopy, which gave valuable insight to the structural, electronic and dynamic properties of these new species when compared to their diamagnetic d^8 and d^{10} valence electron counterparts. However, and at least equally important, these rather accurate data give also rise to puzzling questions which cannot be answered on the basis of relatively simple theories but reveal their limitations. There is a strong demand for more sophisticated treatments. Experiments and calculations in this direction are under way.

Experimental Section

EPR spectroscopy: CW and echo-detected EPR spectra were measured in liquid or frozen THF at S-, X-, Q- and W-band frequencies. The S-band spectra were recorded on a home-built instrument [microwave (mw) frequency 2–4 GHz],[28] the X-band spectra on a Bruker ESP300 spectrometer (mw frequency 9.48 GHz), the Q-band spectra on a home-built instrument (mw frequency 35.3 GHz)[29] and the W-band spectra on a Bruker E680 spectrometer (mw frequency 94.34 GHz). For the X-band spectra the spectrometer was equipped with a liquid nitrogen cyrostat and for the S-, Q- and W-band spectra with a helium cryostat from Oxford Inc. The magnetic fields were measured with a Bruker 035M NMR gaussmeter and 2,2-diphenyl-1-picrylhydrazyl (g value 2.0036) was used as a calibration standard at X-band.

CW EPR spectra at X- and Q-band were measured with a mw power of 20 mW, a modulation frequency of 100 kHz and a modulation amplitude of 0.1 mT and 0.4 mT for the X- and Q-band spectra, respectively. Echo-detected EPR spectra were recorded at S-, Q- and W-band frequencies by using the sequence $\pi/2$-τ-π-τ-echo. To eliminate line-shape distortions due to unwanted field-dependent echo-modulations spectra were recorded with different τ values and added. The following mw pulse lengths, τ values and time increments $\Delta\tau$ were used. S-band: $t_{\pi/2} = 20$ ns, $t_\pi = 40$ ns, $\tau = 380$ to 580 ns in steps of $\Delta\tau = 40$ ns; Q-band: $t_{\pi/2} = 40$ ns, $t_\pi = 80$ ns, $\tau = 100$ to 400 ns in steps of $\Delta\tau = 100$ ns; W-band: $t_{\pi/2} = 100$ ns, $t_\pi = 200$, $\tau = 100$ to 300 ns in steps of $\Delta\tau = 100$ ns.

The HYSCORE and pulse ENDOR spectra were measured at X-band frequency on a Bruker ESP380 spectrometer (mw frequency 9.73 MHz) equipped with a helium cryostat from Oxford Inc. Measurements were done in frozen THF at a temperature of 20 K and a repetition time of 2 ms. The following pulse schemes have been applied.[14]

HYSCORE: HYSCORE experiments were carried out by using the pulse sequence $\pi/2$-τ-$\pi/2$-t_1-π-t_2-$\pi/2$-τ-echo with mw pulse lengths of $t_{\pi/2} = t_\pi =$ 16 ns, a starting time of 96 ns for t_1 and t_2 and time increments of $\Delta t = 16$ ns (data matrix 512×512); an eight-step phase cycle was used. Blind spots were avoided by adding the spectra measured with τ values of 120, 160, 240 and 300 ns.

  0947-6539/02/0803-0608 $ 17.50+.50/0 *Chem. Eur. J.* **2002**, *8*, No. 3

One-dimensional combination-peak experiment: In the one-dimensional combination-peak experiment the echo intensity was measured as a function of time $t_1 = t_2$ incremented from 98 to 4194 ns in steps of 8 ns. To avoid blind spots 64 spectra recorded with τ values between 96 and 704 ns in step of 8 ns were recorded. Fourier transformation of these traces gives the hyperfine axis ν_{hf}.

Davies–ENDOR: Experiments were carried out by using the pulse sequence π-*T*-$\pi/2$-τ-π-τ-echo, with mw pulse lengths of $t_\pi = 160$ ns and $t_{\pi/2} = 80$ ns, $\tau = 240$ ns and a selective radio frequency (rf) pulse of length 9 μs and variable frequency applied during the time interval *T*.

Two-dimensional Mims–ENDOR: Experiments were carried out by using the pulse sequence $\pi/2$-τ-$\pi/2$-*T*-$\pi/2$-τ-echo, with mw pulse lengths of $t_{\pi/2} =$ 16 ns, a selective rf pulse of length 9 μs and variable frequency applied during the time interval *T*. Time τ was varied from 96 ns to 2976 ns in steps of 16 ns. Fourier transformation along this dimension gives the hyperfine axis ν_{hf}.

Data manipulation: Data processing was done with MATLAB (The MathWorks, Inc.). The time traces of the two-dimensional Mims–ENDOR, HYSCORE and combination peak experiment were baseline corrected by using a third-order polynomial, apodized with a Hamming window, zero-filled and then after Fourier transformation the absolute-value spectra were calculated. To remove blind spots and deadtime-dependent distortions in both the HYSCORE and the combination peak data, spectra measured at different τ values were added. Simulations of the CW and echo-detected EPR and the ENDOR data were accomplished with the EasySpin package.[32]

Syntheses—general techniques: All syntheses were performed in carefully dried glassware under an argon atmosphere, which was passed through the Oxisorb® gas purification system (Messer–Griesheim) to remove the last traces of oxygen and moisture. All solvents were dried and purified by using standard procedures and were freshly distilled under argon from sodium/benzophenone (THF), from sodium/diglyme/benzphenone (hexane) or calcium hydride (acetonitrile) prior to use. Air-sensitive compounds were stored and weighed in a glove box (Braun MB 150 B-G system), and reactions on small scale were performed directly in the glove box.

NMR spectra were either taken on an AMX-500, Avance DRX-400, Avance DPX-300 or Avance DPX-250 systems. The chemical shifts are given as dimensionless δ values and were referenced against tetramethylsilane (TMS) for ^{1}H and ^{13}C, 85% H_3PO_4 for ^{31}P, and $CFCl_3$ for ^{19}F NMR spectra. Coupling constants *J* are given in Hz as positive values regardless of their real individual signs. The multiplicity of the signals is indicated as s, d, t, q, sept or m for singlets, doublets, triplets, quartets, septets or multiplets, respectively. Quaternary carbons are indicated as C_{quart}, aromatic as C_{ar}, alkylic as C_{alk} when not noted otherwise. IR spectra were measured with the ATR-technique on a Perkin–Elmer 2000 FT-IR spectrometer in the range from 4000 cm^{-1} to 550 cm^{-1} by using a KBr beamsplitter. The UV/Vis spectra were measured with the UV/Vis/NIR Lambda 19 spectrometer in 0.5 cm quartz cuvettes. Mass spectra were taken on a Finnigan MAT SSQ 7000 in the EI (70 eV) mode.

Synthesis of [CoCl(tropp^{ph})(PPh$_3$)] (6): The bright green complex $[CoCl(PPh_3)_3]$ **5**[33] (0.8 g, 1 mmol) was suspended in THF in a 100 mL flask and then tropp^{ph} (0.4 g, 1 mmol) was added. The reaction mixture slowly turned brown-red. After stirring at room temperature for 8 h, the solvent was evaporated and the brown residue was washed several times with *n*-hexane and then dissolved in a minimum amount of acetonitrile at 40 °C. Upon cooling, deep brown-red crystals precipated which were dried in vaccum (0.6 g, 83%). Elemental analysis calcd (%) for $C_{45}H_{36}ClCoP_2$ (733.11): C 73.73, H 4.95; found: C 73.81, H 4.97; m.p. (decomp) > 195 °C.

Synthesis of [Co(tropp^{ph})$_2$] (7): In a 100 mL flask equipped with reflux condenser and magentic stirring bar, anhydrous cobalt(II) chloride (0.2 g, 1.5 mmol) and tropp^{ph} (1.2 g, 3.2 mmol) were dissolved in THF (30 mL) and subsequently zinc powder (0.5 g, 8 mmol) was added. The reaction mixture was heated under reflux of the solvent for about 45 min. The initially blue colour of the solution turned first olive green, then a red-brown precipitate formed. The reaction mixture was filtred hot and the insoluble material was extracted several times with hot THF. Upon cooling, complex **7** (1.03 g, 85%) crystallised in form of strongly reflecting red-brown crystals. Elemental analysis calcd (%) for $C_{54}H_{42}CoP_2$ (811.82): C 79.89, H 5.21; found: C 79.91, H 5.24; m.p. 207–210 °C; UV/Vis (THF): $\lambda_{max} = 285$, 350 nm.

5,5-Dideutero-10,11-tetradeutero-dibenzo[a,d]cycloheptane (9): Palladium on charcoal (250 mg, 5%) was added to a solution dibenzo[a,d]cycloheptane (5.82 g, 30 mmol) in [D$_1$]actetic acid (50 mL) in a 250 mL pressure glass flask equipped with a teflon cock. The flask was slowly cooled in liquid nitrogen to −196 °C, evacuated (10^{-3} Torr) and then flooded with D_2 to atmospheric pressure. After about 5 min, the temperature was equilibrated at −196 °C and the flask was closed, placed behind a protection wall and slowly warmed to 80 °C, whereby a pressure of about 4.6 atm was build up. After vigorous stirring over night, the pressure was expanded to 1 atm, the reaction mixture was filtered and the solvent distilled off. This procedure was repeated two times and the crude reaction product was finally sublimed at 40 °C in a stationary vacuum to give of **9** (5.46 g, 90%; deuterium content 93%). M.p. 57 °C; ^{1}H NMR ($CDCl_3$): $\delta = 7.52–7.28$ (m, 8H; CH_{ar}), 4.37 (br s, 0.14H; ArC$H_{(7\%)}$(D)$_2$Ar), 3.39 (br s, 0.28H; C$H_{(7\%)}$(D)$_2$C$H_{(7\%)}$(D)$_2$); ^{13}C NMR ($CDCl_3$): $\delta = 139.3$ (2C, C_{quart}), 139.1 (2C, C_{quart}), 129.5 (2C, CH_{ar}), 128.9 (2C, CH_{ar}), 126.6 (2C, CH_{ar}), 126.0 (2C, CH_{ar}), 40.6 (m, 1C, CD_2), 31.9 (m, 2C, CD_2). MS: *m*/*z* (%): 200 (100) [*M*]$^+$, 182 (62), 119 (36); IR: $\tilde{\nu} = 3060$ (w), 3007 (w), 2933 (w), 2204 (w, C–D), 2090 (w, C–D), 1571 (w), 1487 (m), 1440 (w), 1450 (w), 1292 (w), 1115 (w), 1049 (w), 1028 (w), 950 (m), 876 (w), 817 (m), 732 (vs), 682 (w), 611 (m), 582 cm^{-1} (w).

5-Diphenylphosphanyl-5-deutero-10,11-tetradeutero-dibenzo[a,d]cycloheptane (10): *n*BuLi (6.5 mL of a 1.6 M solution in hexanes 10.4 mmol) was added to a solution of **9** (2.00 g, 10 mmol) in dry THF (100 mL) at −20 °C. After one hour stirring at 0 °C, the deep red solution was cooled to −78 °C and titrated with a solution Ph_2PCl (2.3 g, 10.5 mmol) in THF (10 mL) until the red colour disappeared. Precipitates were filtered off, the solvent evaporated in vacuum and the crude product recrystallised from acetonitrile to give **10** as colourless needles (2.83 g, 74%). M.p. 128 °C; ^{1}H NMR ($CDCl_3$): $\delta = 7.43–7.35$ (m, 4H; CH_{ar}), 7.31–7.21 (m, 6H; CH_{ar}), 7.13 (ddd, $^3J_{HH} = 7.7$ Hz, $^4J_{HH} = 1.5$ Hz, $^4J_{HH} = 0.5$ Hz, 2H; CH_{ar}), 7.05 (tt, $^3J_{HH} =$ 7.3 Hz, $^4J_{HH} = 1.5$ Hz, 2H; CH_{ar}), 6.82 (tdd, $^3J_{HH} = 7.7$ Hz, $^4J_{HH} = 1.5$ Hz, $^4J_{HH} = 0.6$ Hz, 2H; CH_{ar}), 6.67 (dt, $^3J_{HH} = 7.5$ Hz, $^4J_{HH} = 1.4$ Hz, 2H; CH_{ar}), 4.15 (br s, 0.07H; CH(D)$_{(7\%)}$P), 2.94 (br s, 0.28H; CH(D)$_{2(7\%)}$); ^{13}C NMR ($CDCl_3$): $\delta = 140.2$ (2C, C_{quart}), 137.9 (2C, $J_{PC} = 10.5$ Hz, C_{quart}), 136.8 (2C, $J_{PC} = 20.6$ Hz, C_{quart}), 134.2 (4C, $J_{PC} = 20.1$ Hz, CH_{ar}), 131.4 (2C, $J_{PC} =$ 3.0 Hz, CH_{ar}), 130.6 (2C, CH_{ar}), 128.9 (2C, CH_{ar}), 128.1 (4C, $J_{PC} = 7.0$ Hz, CH_{ar}), 126.7 (2C, $J_{PC} = 1.5$ Hz, CH_{ar}), 125.4 (2C, CH_{ar}), 32.9 (m, 2C, CD_2), the benzylic carbon (CHP) was not detected; ^{31}P NMR ($CDCl_3$): $\delta = 1.3$ (t, $^2J_{PD} = 6.7$ Hz); MS: *m*/*z* (%): 382 (85) [*M*]$^+$, 197 (100) [[D$_5$]dibenzotropane]$^+$, 183 (84), 168 (44), 118 (80); IR: $\tilde{\nu} = 3015$ (w), 1585 (w), 1484 (m), 1435 (m), 1093 (w), 1027 (w), 999 (w), 742 (vs), 694 (vs), 637 (w), 616 (w), 585 cm^{-1} (w).

Synthesis of *cis*/*trans*-[D$_6$][Rh(tropp^{ph})$_2$]PF$_6$ (*cis*/*trans*-[D$_6$]-1): $[Rh(cod)_2]PF_6$ (115 mg, 0.30 mmol) and **10** (230 mg, 0.62 mmol) were heated to 60 °C in THF (20 mL) for about 16 h. During this time, a microcrystalline red precipitate formed which was filtered, washed several times with *n*-hexanes, and finally dried under vacuum to give 210 mg (70%) of a red powder. The *cis*/*trans* ratio in dichloromethane solution was determined as 80% *trans* and 20% *cis*. M.p. 208–212 °C (decomp); ^{31}P NMR (CD_2Cl_2): $\delta = 85.6$ (d, $^1J_{RhP} = 178$ Hz, *cis*), 84.2 (d, $^1J_{RhP} = 132$ Hz, *trans*), −143.0 (sept, $^1J_{PF} = 712$ Hz, PF_6^-). Further NMR on the fully protonated complex $[Rh(tropp^{ph})_2]PF_6$ data are given in ref. [12]; UV/Vis (THF): $\lambda_{max} = 307$ nm; IR: $\tilde{\nu} = 2955$ (w), 1597 (w), 1484 (w), 1436 (w), 1312 (w), 1186 (w), 1161 (w), 1100 (w), 999 (w), 974 (w), 829 (vs, PF_6^-), 767 (m), 750 (m), 715 (m), 695 (m), 640 (w), 619 (w), 556 cm^{-1} (s).

Synthesis of *cis*/*trans*-[D$_6$][Ir(tropp^{ph})$_2$][O$_3$SCF$_3$] *cis*/*trans*-[D$_6$]-2): $[Ir(cod)_2][O_3SCF_3]$ (110 mg, 0.2 mmol) and **10** (155 mg, 0.4 mmol) were dissolved in THF (10 mL) and subsequently heated 30 min to 80 °C, whereby the initially intense red solution turned pale pink, which indicates the formation of $[D_6][IrD_2(tropp^{ph})_2][O_3SCF_3]$ (**11**).[17] This complex was transformed into the colourless complex $[D_6][Ir(NCMe)(tropp^{ph})_2]$-$[O_3SCF_3]$ (**12**) by adding acetonitrile (10 mL). All volatiles were evaporated and the remaining solid was dried for 4 h at 100 °C under vacuum (10^{-3} Torr) and then dissolved in CH_2Cl_2, which turned burgundy red. The product was precipitated with *n*-hexane to give an olive-green powder in 93% yield (*trans*/*cis* ratio = 88:12). M.p.(decomp.) 275–277 °C; ^{1}H NMR (CD_2Cl_2): $\delta = 7.82$ (dd, $^3J_{HH} = 7.6$ Hz, $^4J_{HH} = 1.2$ Hz, 2H; C$H_{ar,cis}$), 7.55 (t, $^3J_{HH} = 7.6$ Hz, 2H; C$H_{ar,trans}$), 7.42 (t, $^3J_{HH} = 7.9$ Hz, 4H; C$H_{ar,trans}$), 7.35–7.25 (m, CH_{ar}), 7.21 (td, $^3J_{HH} = 7.7$ Hz, $^4J_{HH} = 2.2$ Hz, 2H; C$H_{ar,trans}$), 7.14 (td, $^3J_{HH} = 7.7$ Hz, $^4J_{HH} = 1.2$ Hz, 2H; C$H_{ar,cis}$), 7.10–7.02 (m, CH_{ar}), 7.00 (dd, $^3J_{HH} = 7.7$ Hz, $^4J_{HH} = 1.0$ Hz, 2H; C$H_{ar,trans}$), 6.84 (br d, $^3J_{HH} = 7.7$ Hz, 2H;

$CH_{ar,trans}$), 6.80 (td, $^3J_{HH}=8.2$ Hz, $^4J_{HH}=2.0$ Hz, 4H; $CH_{ar,cis}$), 6.55 (br t, $^3J_{HH}=9.3$ Hz, 4H; $CH_{ar,cis}$), 6.05 (d, $^3J_{PH}=2.2$ Hz, 2H; C=$CH_{(7\%)}$(D)), 5.97 (t, $^3J_{PH}=3.6$ Hz, 2H; C=$CH_{(7\%)}$(D)), 5.34 (t, $^2J_{PH}=3.2$ Hz, 2H; $CH_{(7\%)}(D)P_{trans}$). The signals of the not-exchanged olefinic and benzylic CHP protons of the *cis* isomer were not detected because of their low intensity (i.e. 7% of 12%); ^{13}C NMR (CD_2Cl_2): δ (*trans*) = 137.5 (t, $J_{PC}=$ 4.8 Hz, 4C, C_{quart}), 134.4 (t, $J_{PC}=5.5$ Hz, 8C, CH_{ar}), 134.0 (m, 4C, C_{quart}), 132.7 (4C, CH_{ar}), 133.2 (4C, C_{quart}), 131.6 (4C, CH_{ar}), 129.8 (t, $J_{PC}=4.9$ Hz, 8C, CH_{ar}), 129.6 (4C, CH_{ar}), 129.4 (4C, CH_{ar}), 129.3 (4C, CH_{ar}), 70.5 (br m, 4C, =CD), 50.8 (br m, 2C, DCP); ^{31}P NMR (CD_2Cl_2): $\delta=72.8$ (*trans*), 68.8 (*cis*); UV/Vis (CH_2Cl_2): $\lambda_{max}=494$, 363 nm; IR: $\tilde{\nu}=3048$ (w), 2878 (w), 1484 (w), 1438 (m), 1313 (w), 1257 (vs, SO_3^-), 1222 (m), 1152 (m), 1098 (m), 1055 (m), 1028 (w), 1000 (s), 794 (w), 766 (w), 744 (m), 712 (m), 692 (s), 635 cm^{-1} (s).

General synthesis of the paramagnetic complexes [M(tropp^{ph})$_2$] by a symproportion reaction from [M(tropp^{ph})$_2$]$^+$A$^-$ and [M^1(THF)$_n$]$^+$-[M(tropp^{ph})$_2$]$^-$ (M = Rh: 3 and [D$_6$]-3; M = Ir: 4 and [D$_6$]-4; [M^1(THF)$_n$]$^+$ = [K(THF)$_6$]$^+$ or [Li(THF)$_4$]$^+$): The following procedure proved to be the most simple for the preparation of pure quantities of the paramagnetic complexes **3**, [D$_6$]-**3**, **4** and [D$_6$]-**4** (see also refs. [12, 13]). A precisely measured amount of the cationic 16-electron complexes [M(tropp^{ph})$_2$]$^+$A$^-$ (M = Rh, A = PF_6^-: **1** or [D$_6$]-**1**; M = Ir, A$^-$ = $CF_3SO_3^-$: **2** or [D$_6$]-**2**) was suspended in THF and a small shiny piece of an alkali metal was added. After some time (~30 min) the reaction mixture turned from red to brown to green to red-brown and finally to deep red. In course of the reaction the starting material was completely dissolved and a clear solution was obtained which contained the d^{10}-metalates [M(tropp^{ph})$_2$]$^-$ (with quantities of about 100 mg of **1** or **2**, the reactions are usually complete within 4 h). Subsequently, precisely one equivalent of the cationic [M(tropp^{ph})$_2$]$^+$A$^-$ complexes was added to the reaction mixture which immediately turned deep green. When sodium or potassium were used as reducing agents, the reaction mixture was filtered to remove the alkali salts, [M^1]$^+$[A]$^-$. This procedure is of advantage when A$^-$ = PF_6^- and was used here for the synthesis of [D$_6$]-**3**. When lithium was used, the corresponding salts were left in solution, especially when A$^-$ = $CF_3SO_3^-$ and this method was applied here for the synthesis of [D$_6$]-**4**. The addition of *n*-hexanes (about one third of the volume which was used for the reaction) led to the precipitation of deep green (almost black) crystals, which were collected after 16 h, washed with *n*-hexanes and dried in vacuum. Yields of 60–80% were obtained for [D$_6$]-**3** (UV/Vis (THF): $\lambda_{max}=491$, 478, 450, 419 nm) and yields of 70–90% for [D$_6$]-**4** (UV/Vis (THF): $\lambda_{max}=592$ nm). Further physical data are given in Table 1 and refs. [12, 13].

Acknowledgements

We thank Dr. A. Kamlowski from Bruker GmbH, Karlsruhe, for the W-band measurements. This research has been supported by the Swiss National Science Foundation. We thank Dipl.-Chem. S. Loss for performing the X-ray analyses.

[1] a) R. Poli, *Chem. Rev.* **1996**, *96*, 2135 and references therein; b) A short overview on rhodium(0) and iridium(0) complexes is given in: S. Deblon, H. Rüegger, H. Schönberg, S. Loss, V. Gramlich, H. Grützmacher, *New J. Chem.* **2001**, *25*, 83.

[2] a) E. Muetterties, J. Blecke, Z.-Y. Yang, V. Day, *J. Am. Chem. Soc.* **1982**, *104*, 2940; b) H.-F. Klein, M. Helwig, U. Koch, G. Lull, M. Tadic, C. Krüger, P. Hofmann, *Z. Naturforsch. Teil. B* **1988**, *43*, 1427; c) J. Chenier, M. Histed, J. Howard, H. Joly, H. Morris, B. Mile, *Inorg. Chem.* **1989**, *28*, 4114, and references therein; d) L. Hanlan, H. Huber, E. P. Kündig, B. R. McGarvey, G. A. Ozin, *J. Am. Chem. Soc.* **1975**, *97*, 7054; e) [Rh(CO)$_x$] ($x=1-4$) were previously investigated by: G. A. Ozin, A. J. L. Hanlan, *Inorg. Chem.* **1979**, *18*, 2091; f) A. B.P Lever, G. A. Ozin, A. J. L. Hanlan, W. J. Power, H. B. Gray, *Inorg. Chem.* **1979**, *18*, 2088.

[3] a) G. George, S. Klein, J. Nixon, *Chem. Phys. Lett.* **1984**, *108*, 627; b) G. Pilloni, G. Zotti, S. Zecchin, *J. Organomet. Chem.* **1986**, *317*, 357.

[4] G. Zotti, S. Zecchin, G. Pilloni, *J. Electroanal. Chem.* **1984**, *175*, 241.

[5] G. Zotti, S. Zecchin, G. Pilloni, *J. Organomet. Chem.* **1983**, *246*, 61.

[6] J. Orsini, W. E. Geiger, *J. Electroanal. Chem.* **1995**, *380*, 83.

[7] B. Longato, L. Riello, G. Bandoli, G. Pilloni, *Inorg. Chem.* **1999**, *38*, 2818.

[8] H. A. Jahn, E. Teller, *Proc. R. Soc. London Ser. A* **1937**, *161*, 220.

[9] H.-F. Klein, M. Helwig, M. Karnop, H. König, B. Hammerschmitt, G. Cordier, U. Flörke, H.-J. Haupt, *Z. Naturforsch. Teil B* **1993**, *48*, 785.

[10] K. A. Woods, J. C. Bart, M.Calcaterra, G. Agnès, *Organometallics* **1983**, *2*, 627; b) see also: M. D. Athar Masood, P. S. Zacharias, *Polyhedron* **1991**, *10*, 811.

[11] J. Thomaier, S. Boulmaâz, H. Schönberg, H. Rüegger, A. Currao, H. Grützmacher, H. Hillebrecht, H. Pritzkow, *New J. Chem.* **1998**, *21*, 947.

[12] H. Schönberg, S. Boulmaâz, M. Wörle, L. Liesum, A. Schweiger, H. Grützmacher, *Angew. Chem.* **1998**, *109*, 1492; *Angew. Chem. Int. Ed.* **1998**, *37*, 1423.

[13] H. Grützmacher, H. Schönberg, S. Boulmaâz, M. Mlakar, S. Deblon, S. Loss, M. Wörle, *Chem. Commun.* **1998**, 2623.

[14] A. Schweiger, G. Jeschke, *Principles of Pulse Electron Paramagnetic Resonance*, Oxford University Press, Oxford, **2001**.

[15] Compound **6**: triclinic, space group $P\bar{1}$; $a=9.9018(15)$, $b=12.059(2)$, $c=15.754(2)$ Å, $\alpha=83.7520(10)$, $\beta=89.7490(10)$, $\gamma=77.697(2)^\circ$; $V=1826.6(5)$ Å^3; $Z=2$, $Mo_{K\alpha}$ radiation, $2\Theta_{max}=49.5^\circ$. 12021 reflections, 6242 independent ($R_{int}=0.0571$); $R_1=5.68\%$, w$R_2=14.10\%$ (based on F^2) for 442 parameters and 6241 reflections with $I>2\sigma(I)$. The structure was solved by direct methods and was refined against full matrix (versus F^2) with SHELXTL (Version 5.0). Crystallographic data (excluding structure factors) for the structure reported in this paper have been deposited with the Cambridge Crystallographic Data Centre as supplementary publication no. CCDC-161438. Copies of the data can be obtained free of charge on application to CCDC, 12 Union Road, Cambridge CB2 1EZ, UK (fax: (+44) 1223-336-033; e-mail: deposit@ccdc.cam.ac.uk). Compound **7**: triclinic, space group $P\bar{1}$; $a=11.365(2)$, $b=12.257(3)$, $c=17.116(3)$ Å, $\alpha=98.50(3)$, $\beta=100.37(3)$, $\gamma=105.40(3)^\circ$; $V=2212.5(8)$ Å^3; $Z=2$, $Mo_{K\alpha}$ radiation, $2\Theta_{max}=48.3^\circ$. 12251 reflections, 6281 independent ($R_{int}=0.2341$); $R_1=18.57\%$, w$R_2=44.82\%$ (based on F^2) for 244 parameters and 6270 reflections with $I>2\sigma(I)$. The structure was solved by direct methods and was refined against full matrix (versus F^2) with SHELXTL (Version 5.0). Due to the poor quality, the crystallographic data were not deposited but are available from the authors upon request.

[16] A. G. Orpen, L. Brammer, F. H. Allen, O. Kennard, D. G. Watson, *J. Chem. Soc. Dalton Trans.* **1989**, S1.

[17] C. Böhler, N. Avarvari, H. Schönberg, M. Wörle, H. Rüegger, H. Grützmacher, *Helv. Chim. Acta* **2001**, *84*, 3127.

[18] Selected literature on dehydrogenations of alkanes by iridium complexes: a) R. H. Crabtree, M. Lavin, *J. Chem. Soc. Chem. Commun.* **1985**, 794; b) R. H. Crabtree, C. P. Parnell, *Organometallics* **1985**, *4*, 519; c) T. Aoki, R. H. Crabtree, *Organometallics* **1993**, *12*, 294; d) M. J. Burk, R. H. Crabtree, *J. Am. Chem. Soc.* **1987**, *109*, 8025; e) R. H. Crabtree, C. P. Parnell, R. J. Uriarte, *Organometallics*, **1987**, *6*, 696; f) M. Prinz, M. Grosche, E. Herdtweck, W. A. Herrmann, *Organometallics* **2000**, *19*, 1692; g) A short review on metal promoted alkane dehydrogenations is given by: C. M. Jensen, *Chem. Commun.* **1999**, 2443.

[19] Although this was not reported in references [12, 13], the same isomer ratios are obtained when **1** and **2** are prepared in reactions with tropp^{ph} and [M(cod)$_2$][O_3SCF_3] or [M$_2$(μ_2-Cl)$_2$(cod)$_2$]/AgO_3SCF_3.

[20] W. B. Mims, *Proc. R. Soc. London Ser. A* **1965**, *283*, 452.

[21] K. T. Mueller, A. J. Kunin, S. Greiner, T. Henderson, R. W. Kreilick, R. Eisenberg, *J. Am. Chem. Soc.* **1987**, *109*, 6313.

[22] T. A. Albright, J. K. Burdett, M.-H. Whangbo, *Orbital Interactions in Chemistry*, Wiley, New York **1984**, 304. In a forecoming paper we will show, that very likely pentacoordinate complexes are not involved in the *trans*–*cis* isomerisations of **3** and **4**; however, such species are responsible for the isomerisation of the cations **1** and **2** in coordinating solvents.

[23] P. Höfer, A. Grupp, H. Nebenführ, M. Mehring, *Chem. Phys. Lett.* **1986**, *132*, 279.

[24] A. Pöppl, L. Kevan, *J. Phys. Chem.* **1996**, *100*, 3387.

[25] A. K. Koh., D. J.Miller, *At. Data Nucl. Data Tables* **1985**, *33*, 235.

[26] a) M. L. Munzarova, P. Kubacek, M. Kaupp, *J. Am. Chem. Soc.* **2000**, *122*, 11900.

  0947-6539/02/0803-0610 $ 17.50+.50/0 *Chem. Eur. J.* **2002**, *8*, No. 3

[27] B. A. Goodman, J. B. Raymor, in *Advances in Inorganic Chemistry and Radiochemistry* (Eds.: H. J. Emeléus, A. G. Sharpe), Academic Press, New York, **1970**.
[28] M. Willer, J. Forrer, J. Keller, A. Schweiger, *Rev. Sci. Instrum.* **2000**, *71*, 2807.
[29] I. Gromov, J. Shane, J. Forrer, R. Rakhmatoullin, Yu. Rozentzwaig, A. Schweiger, *J. Magn. Reson.* **2001**, *149*, 196.
[30] C. A. Bates, W. S. Moore, K. J. Standley, K. W. Stevens, *Proc. Phys. Soc.* **1962**, *79*,73.
[31] S. A. Fairhurst, J. R. Morton, K. F. Preston, *J. Magn. Reson.* **1983**, *55*, 453.
[32] See the website http://www.esr.ethz.ch/research/EasySpin/home.html
[33] S. L. Baysdon, L. S. Liebeskind, *Organometallics* **1982**, *1*, 771.

Received: July 10, 2001 [F3404]